Shear and tensile joint strengths of carbon fiber-reinforced thermoplastics using ultrasonic welding

Keita Goto[a,*], Kenta Imai[a], Masahiro Arai[a], Takashi Ishikawa[b]

[a] *Department of Aerospace Engineering, Nagoya University, Furo-cho, Chikusa-ku, Nagoya, 464–8603, Japan*
[b] *National Composites Center Japan, Nagoya University, Furo-cho, Chikusa-ku, Nagoya, 464–8603, Japan*

Abstract

The shear and tensile strengths of carbon fiber-reinforced thermoplastic (CFRTP) laminate joints by ultrasonic welding were investigated by lap shear tests (LSTs) and cross tensile tests (CTTs). The adherends were the cross-ply and the twill woven CFRTP laminates, and the flat energy director (FED) was used to clarify its effectiveness. A modified jig and testing method for CTTs were newly proposed. In each test, the strengths were calculated in two ways: by indicators of "welding efficiency" and "welding quality." From the experimental results, the strengths of the cross-ply laminate joints were saturated at high welding energy, and the "welding quality" was improved by FED. On the other hand, higher strengths of the twill woven laminate joints were obtained as the welding energy increased, and the effectiveness of FED was confirmed mainly for the "welding efficiency." The fracture surfaces were then observed to clarify the fracture mechanisms of the joints.

Keywords: A. Polymer-matrix composites (PMCs), B. Strength, E.

*goto@nuae.nagoya-u.ac.jp

1. Introduction

Recently, carbon fiber-reinforced thermoplastics (CFRTPs) have attracted much attention as a next-generation structural material. Moreover, CFRTPs have high productivity compared with epoxy-based carbon fiber-reinforced thermosetting plastics (CFRTSs) because they can be formed by injection molding and press molding quickly. Thus, CFRTPs are expected to be applicable to not only high-end but also mass-produced products such as popularly priced cars [1, 2, 3]. However, the assemby methods of CFRTP structural parts are important because it is difficult to form large structures with complex shapes by press molding.

Assembly methods such as mechanical joints using bolts or rivets, and chemical bonding by adhesives, are generally used in the engineering field. However, these methods have some problems or disadvantages, for instance, stress concentrations around bolt or rivet halls, increases in structural weight owing to joint components, or long curing time of adhesives. As for CFRTP structures, welding techniques are applicable as the assembly method. Welding techniques are suitable for mass-produced items because they can be processed quickly without any consumables. Some types of welding techniques for CFRTPs are ultrasonic, laser [4], electromagnetic induction [5], and resistance welding [6, 7]. These have been investigated in order to realize higher strength and quality of welded joints.

In particular, ultrasonic welding has some attractive advantages, for example short welding time, low power consumption, and ease of automation.

Ultrasonic welding can be applied to joints of various thermoplastic materials, including dissimilar joints such as CFRTP-CFRTS [8], CFRTS-CFRTS with a thermoplastic coupling layer [9], and CFRTP- or CFRTS-metal joints [10, 11]. In addition, ultrasonic welding can perform in situ monitoring during the welding process, for example displacement of the sonotrode, vibration time, dissipated power, and welding energy and force. Welding parameter optimization based on this process data has been investigated [12, 13]. Villegas found that the vibration phase in the welding process can be divided into five stages by the characteristics of the time histories of dissipated power and sonotrode displacement [14]. Villegas also investigated the relation between the joint strength and each vibration phase of the welding [15]. According to the literature, the maximum strength of the joints can be obtained when the facing surfaces of the adherends begin to melt.

However, the quality of the joints by ultrasonic welding is strongly affected by the surface condition of the adherends. The surface roughness of the adherends causes nonuniform contact, which can lead to variations in the welded areas or degradation of the joint strength. For this, an energy director (ED), which concentrates ultrasonic heating at the welding surface, is usually formed at the adherend surfaces. ED plays an important role in realizing stable welding quality [16].

The general shapes of EDs are liner ridges with semicircular, rectangular, or triangular cross sections [17]. In addition, a complex-shaped ED using microsphere composite films has also been developed to solve the problems of variations in the welding layer thickness, the flow of a melted matrix, and the presence of trapped air [18]. However, it needs enough consideration to

design of ED because the joint strength is affected by the shape, size, and direction of the ED's pattern [19]. To simplify the design process for ED, a flat energy director (FED) has been proposed. FED is easily molded on the adherend surfaces like a resin-rich layer using thermoplastic neat films, and heat generation at the welding surface is promoted owing to differences in stiffness between the adherends and FED. In addition, FED shows almost the same strength as the ridge-shaped ED [20]. Thus, FED is considered to be suitable for joint structures of mass production. Some numerical simulations have also been performed to understand the welding processes in detail. However, the numerical simulations of ultrasonic welding require complex numerical methods considering multiphysics problems consisting of viscoelastic, flow, and heating factors. Levy et al. analyzed the displacement and adhesion of the traditional ED and FED during ultrasonic welding [21, 22].

As mentioned previously, many experimental and numerical studies on ultrasonic welding have been reported. In the engineering field, however, ultrasonic welding has rarely been used to assemble CFRTP structures. One of the reasons is insufficient information for the welding parameters, for example, the suitable welding energy and the effect of ED. In addition, the strength of the CFRTP joints is mainly evaluated only by lap shear tests and few studies on the tensile strength of the joints have been reported. Zhao et al. investigated the strength and stiffness of spot-welded CFRTP joints and compared them with those of mechanically fastened joints by using double-lap shear and pull-through tests [23]. The researchers revealed that the stiffness and shear strength of spot-welded joints are almost the same as or higher than those of mechanically fastened joints, but the tensile

strength of welded joints is inferior to that of mechanical joints because no reinforcement exists for the out-of-plane direction of the welded joints. As for the industrial viewpoint, it is very important to evaluate not only the shear but also the tensile strength.

However, out-of-plane tensile tests for CFRTP joints are complex compared with lap shear tests. On the one hand, the pull-through test is standardized in ASTM D7332-09, where two square composite plates with four drilled holes are required. On the other hand, cross tensile tests are generally used for metal-metal joints [24, 25]. Cross tensile tests are simple and require relatively small specimens, but some drilled holes are still needed to fix the specimen on the jig. Szlosarek et al. investigated the shear and tensile strengths of flow drill screw joints between CFRTS and an aluminum alloy under pure-shear, pure-tensile, and shear-tensile mixed stress states [26]. They used CFRTS with no fixing holes as the specimen to minimize the notch effect. From the viewpoint of convenience, it is significant to develop an out-of-plane tensile test method that is similar to the cross tensile test but without drilling.

The main objective of the present study is to evaluate the shear and tensile strengths of CFRTP joints by ultrasonic welding with different welding energies. Lap shear and cross tensile tests were performed to obtain the strengths of the joints. A modified CTT jig for CFRTP joints was designed, and a testing method to evaluate the tensile strengths of CFRTP joints was proposed. For the adherends, cross-ply and twill woven CFRTP laminates were used. In addition, the adherends were jointed with and without FED in order to clarify the effectiveness of FED on the strengths. An energy-

controlled welding mode was selected to evaluate the effect of the welding energy on the joint strengths. Furthermore, the welding surfaces were observed using a scanning electron microscope (SEM) after the tests in order to reveal the mechanisms of the shear and tensile fractures of the joints.

2. Ultrasonic welding

2.1. Adherends

The adherends used in this study were cross-ply CFRTP laminates made of unidirectional prepregs and twill woven CFRTP laminates. The unidirectional prepregs used for the cross-ply laminates were TC910 (Ten Cate Advanced Composites), which are composed of the thermoplastic resin polyamide-6 (PA6) and carbon fibers T700S. The stacking sequence of the cross-ply CFRTP laminates was $[0_2/90_2/0_2/90]_S$. The laminates were formed by a table-top press forming machine SA-303 (Tester Sangyo Co., Ltd.) with a press condition of 225 °C and 0.96 MPa for 20 min. This condition was determined to prevent excessive resin flow of the unidirectional prepregs. The nominal thickness of the cross-ply laminates was 2.9 mm. The twill woven laminates were made of 10 sheets of carbon fiber/PA6 twill woven prepreg PA6-3KT1 (Ichimura Sangyo Co., Ltd.). The forming temperature and time were the same as those of the cross-ply laminates at 225 °C and 20 min, but the forming pressure was determined as 2.4 MPa to avoid interlaminar voids. The nominal thickness of the twill woven laminates was 2.7 mm. The fiber volume fraction of each laminate was approximately 50%. The relation between the stress and strain of the cross-ply and twill woven laminates used in this study is shown in Fig. 1.

A flat energy director (FED) made of PA6 films SHT-N6 (Toray Plastics Precision Co., Ltd.) was used in this study to improve the welding quality of the joints. The thickness of the films was 0.3 mm. Two types of joints (with and without FED) were welded to clarify the effect of FED. FED was molded on the adherends during the forming phase of the laminates. During the welding of the joints with FED, the adherend with FED was set on the lower side, and the other one without FED was set on the upper side, as shown in Fig. 2.

2.2. Welding procedure

The ultrasonic welding machine used in this study consisted of an oscillator JS3600s (Seidensha Electronics Co., Ltd.) and a press machine JP80s (Seidensha Electronics Co., Ltd.). The frequency control system of the oscillator was a digital phase-locked-loop frequency tracking method. The oscillation frequency was 15.15±0.15 kHz. Three welding modes (energy-, time-, and displacement-controlled welding modes) are available in this oscillator. It was reported that the displacement-controlled welding mode has some advantages for the joint quality compared with the other welding modes [15]. However, as long as several types of specimens were tried welding, it seems that the displacement- or energy-controlled welding mode dominated depending on the cases. In this research, it was found that the energy amount has a higher correlation with the strengths than the displacement. As shown in the following section, the depth of indentation was quite different in the cases of the cross-ply and twill woven laminates. Therefore, the energy-controlled welding mode was reasonable to evaluate the the joint strengths of these two types of adherends with the same index. The geometry of the sonotrode tip

was 10 mm × 10 mm square, and the amplitude of the vibration was 90 μm.

In ultrasonic welding, the sinusoidal electrical signal was generated by the oscillator. The ultrasonic signal was then transmitted to a piezoelectric transducer and converted into mechanical vibration. The mechanical vibration energy was applied to the upper surface of the overlapped adherends via the sonotrode, as shown in Fig. 2. The surface friction and viscoelastic energy were generated at the welding surface of the adherends. Since the temperature at the welding surface instantaneously exceeded the melting temperature of the thermoplastic resin, the adherends were welded. During the ultrasonic welding process, a static load was also applied on the adherends by the sonotrode.

There are three main parameters for ultrasonic welding in the energy-controlled welding mode: welding energy, oscillation starting load, and maximum load. In addition, there are the load-increasing and constant-load sequences of the ultrasonic welding, but in this research, as long as the energy-controlled mode is used, it was confirmed that there is no large difference between them. Therefore the load-increasing sequence which is recommended by the manufacturer of the welding machine was selected. Variations of the load and dissipated power in the welding sequence are shown in Fig. 3. A static load was first applied on the adherends by the sonotrode (t_1). When the load reached the oscillation starting load (t_2), ultrasonic vibration was applied to the adherends. The applied load continued to rise to the preset value as the maximum load during vibration, and thereafter it was maintained at a constant value. The applied welding energy was calculated by the time integration of the welding power which is a product of the vibra-

tion displacement and load of the sonotrode. The vibration terminated when the amount of energy applied to the adherends reached the predetermined welding energy (t_3). Finally, the load was statically held for 5 s, and the welding process was completed. The oscillation starting load and the maximum load were, respectively, specified to 400 N and 940 N. In the present study, the strengths of the joints with different welding energies are compared and evaluated to determine the optimal welding condition.

2.3. Experimental methods

2.3.1. Lap shear test

To evaluate the shear strength of the joints, lap shear tests (LSTs) were performed. LSTs are widely performed as an evaluation test of the joint strength because of their convenience [27]. The geometry of the specimens is shown in Fig. 4. The adherends were cut into 82.5 mm × 25.0 mm sections and were overlapped in an area of 25.0 mm × 25.0 mm. The sonotrode contacted the upper adherend at the center of the overlap area of 10.0 mm × 10.0 mm. The fiber orientation on the surface of the adherends made of the cross-ply laminates was parallel to their longitudinal direction. The ultrasonic welding jig of the LST specimens is graphically explained in Fig. 5. A pair of adherends was placed with spacers at the inside of the jig and clamped by fixing tools to avoid movement of the adherends during ultrasonic welding. The adherends of the cross-ply laminates without FED were welded by four welding energies: 200 J, 450 J, 650 J, and 800 J. This was done to investigate suitable range of the welding energy, and it was revealed that 200 J of welding energy was too low to obtain sufficient joint strength, as mentioned in the next section. Thus, three welding energies (450 J, 650 J,

and 800 J) were employed for the other types of adherends. The number of experiments was seven, but the average value and the standard deviation of the strengths were calculated from five results except extremely large and small values.

LSTs were performed according to the ASTM D5868 standard. A universal material testing machine AG-5000B (Shimadzu Corp.) was used, and the crosshead speed was set to 1.0 mm/min. The tests were performed under a standard temperature of 23 °C after drying of the specimens at 80 °C for 16 h using a vacuum oven to avoid the effect of water absorption. Both ends of the specimens were cramped with spacers that had the same thickness as the adherends in order to avoid eccentricity in the specimens.

The lap shear strength (LSS) was calculated in two ways as proposed by Villegas et al [19]. LSS1 is calculated as the maximum load divided by the entire overlap area, while LSS2 is calculated as that divided by the actual welded area. The actual welded area was obtained from fractured surface observations of the joints after the tests. As an example, Fig. 6 shows the fracture surface of the cross-ply laminate joint without FED welded by 800 J. As shown in the figure, the actual welded area can be clearly distinguished from the nonwelded area. The image of the fracture surface of the joint is then binarized, and the ratio of the actual welded area can be obtained. In this case, the ratio of the actual welded area is calculated as 34.0 % of the entire overlap area (625 mm^2). LSS1 and LSS2 are the indicators for "welding efficiency" and "welding quality," respectively.

2.3.2. Cross tensile test

To apply the ultrasonic welding of CFRTPs to industrial structures, the tensile strength of the joints is also important. In the present study, cross tensile tests (CTTs) for CFRTP joints were newly proposed to evaluate the tensile strength (CTS) of the joints.

The geometry of the specimens is shown in Fig. 7. The adherends were cut into 25.0 mm × 50.0 mm sections and were welded to the center of the overlapped area 25.0 mm × 25.0 mm. The fiber orientation on the surface of the adherends of the cross-ply laminates was parallel to their longitudinal direction. Thus, the fibers were crossed orthogonally at the welded surface of the specimens. All adherends were welded at three welding energies: 450 J, 650 J, and 800 J. The average strength and its standard deviation were calculated from five results by seven experiments, as in the LST case. The jig for the ultrasonic welding of the CTT specimens is graphically shown in Fig. 8. The jig was designed to avoid unnecessary movement of the adherends during welding by a groove and fixing tools.

A modified CTT jig for CFRTP joints is shown in Fig. 9(A). The specimen was placed inside of the jig and supported at the edges of the adherends by a simple support to weaken the boundary condition as shown in Fig. 9(B). The testing machine and the conditions were the same as those for the LSTs. CTS was also calculated in two ways in a similar manner to LSS. CTS1 is for the values calculated as the maximum load supported by the joint divided by the entire overlap area, and CTS2 is for the values calculated as that divided by the actual welded area.

3. Experimental results and discussion

3.1. Lap shear test

3.1.1. Welding results

The effects of the welding energy and FED on the welding results, which are the welded area of the joints and the indentation by the sonotrode, were investigated. Fig. 10 shows the calculated welded area of the cross-ply laminate joints. The welded area of the joints without FED are almost the same for all welding energies, and that of the joints with FED are also saturated at 650 J and 800 J. However, the welded area of the joints with FED is smaller than that of the joints without FED. This is because the joints were intensively welded at the area beneath the sonotrode by FED. Then, the depth of indentation by the sonotrode is indicated in Fig. 11. For the joints without FED, the indentation became deep as the welding energy increased, especially at 800 J. Note that smoke occurred during the welding sequence at 800 J. This means that the adherend was overheated and softened by the excessive welding energy, which was not fully consumed at the welding surface. This deep indentation can decrease the mechanical properties of the joints such as the bending strength. By contrast, for the cases of the joints with FED, the indentation welded by 800 J is similar to that welded by 650 J.

The welded area and indentation of the twill woven laminate joints are also shown in Figs. 12 and 13. Compared with the results of the cross-ply laminate joints, the effect of FED is clearly observed because the welded area drastically increased for the joints with FED welded by 800 J. The indentations of the adherend surfaces, however, were relatively shallow compared

with those of the cross-ply laminate joints: about 0.20 mm for all welding conditions. The indentation of the cross-ply and twill woven laminate joints without FED welded at 800 J is illustrated in Fig. 14. A remarkable indentation (0.94 mm) can be observed in the cross-ply laminate joint, while a slight indentation (0.18 mm) was found in the twill woven one. This is because the three-dimensional woven structure of the reinforcing fibers prevents the sonotrode from sinking into the adherends.

3.1.2. Load-displacement curve

The representative load-displacement curves of LSTs for the cross-ply laminate joints with four welding energies are shown in Fig. 15. In the figure, the results of the joints welded with and without FED are indicated by solid and dotted lines, respectively. Although the little nonlinearity of the curves owing to backlash in the testing machine and the jig can be found around 0.2 mm of the displacement, all results showed almost linear behavior, and then the loads decreased drastically. The maximum loads became high as the welding energy increased to 650 J, but almost saturated at more than 650 J in the joints with and without FED. For the cross-ply laminate joints, little effect of FED could be observed as shown in Fig. 15, except for 450 J. This is because the welding energy of 450 J is not enough to weld the joints with FED and this result in a small welded area as shown in Fig. 10. Here, as an example, the individual load-displacement curves of the cross-ply laminate joints with FED welded at 650 J are indicated in Fig. 16. Similar curves can be found on the four specimens, but the slope of the curve for one specimen became small because premature failure of the joint occurred.

Fig. 17 shows the representative load-displacement curves for the twill

woven laminate joints with three welding energies. The maximum loads for the joints welded without FED increased from about 2 kN to 4 kN for 450 J and 650 J, but became almost the same values for 650 J and 800 J, as indicated by the dotted lines in Fig. 17. By contrast, the maximum loads increased with higher welding energies in the case of the joints welded with FED. These are indicated by the solid lines in Fig. 17. Moreover, the effect of FED was clearly observed because the maximum loads of the joints welded with FED showed higher values compared with those welded without FED, especially at 800 J. This is because the twill woven laminates have large surface roughness owing to the woven fabrics compared with the cross-ply laminates. The melting resin from FED can help fill in such roughness. The individual load-displacement curves of the twill woven laminate joints with FED welded at 800 J are shown in Fig. 18. The curves until final fracture are similar for all specimens, but the maximum load and displacement are different for each specimen.

3.1.3. Lap shear strength 1

Fig. 19 shows LSS1 of the cross-ply laminate joints without and with FED. It can be found that LSS1 of the joints without FED welded at 200 J was extremely low but increased drastically from 1.5 MPa to 7.0 MPa with an increase in the welding energy to 650 J, and it slightly decreased when welded at 800 J. In addition, the indentation in the joints welded at 800 J was quite deep compared with that welded at 650 J, as mentioned in Fig. 11. Therefore, it can be determined that 650 J is the efficient welding energy in terms of the joint strength and the joint surface condition. It is noted that a low LSS1 was observed for the joints welded at 200 J, although the welded

area was similar to that of the other conditions. This is because the fracture modes were different between the joints welded at 200 J and the others. No fiber breakage occurred at 200 J. Similarly, LSS1 for the cross-ply laminate joints with FED increased drastically from about 3.3 MPa at 450 J to 7.1 MPa at 650 J, and almost saturated at 650 J and 800 J. Thus, the efficient welding energy for the cross-ply laminate joints with FED is also estimated as 650 J. However, the effectiveness of FED was not sufficiently confirmed for LSS1 for the cross-ply laminate joints because the maximum LSS1 with and without FED was almost the same value, which was approximately 7.0 MPa. The efficient welding energy was identified as 650 J for both joints.

Then, Fig. 20 shows LSS1 of the twill woven laminate joints without and with FED. In contrast to the results of the cross-ply laminate joints, LSS1 steadily increased with an increase in the welding energy for the joints without and with FED. In particular, LSS1 of the joint with FED welded at 800 J showed an extremely high value at 11.5 MPa, which was about twice as high as that of the cross-ply laminate joints or the twill woven laminate ones without FED. From these results, the efficient welding energy for the twill woven laminate joints was presumed to be 800 J, and the effectiveness of FED was confirmed.

3.1.4. Lap shear strength 2

LSS2 of the cross-ply laminate joints without and with FED is shown in Fig. 21. For the cross-ply laminate joints without FED, LSS2 welded at 200 J was still low, and it almost saturated at around 25.0 MPa when welded at 450 J, 650 J, and 800 J. This means that a similar joint quality can be obtained even if the welding energy is increased to higher than 450 J for the

cross-ply laminate joints without FED, and an increase in the welding energy from 450 J contributes only to the welding efficiency and not the quality, thus extending the welding area. Although LSS2 of the joints with FED welded at 450 J had similar values as that of the joints without FED, it increased to about 40.0 MPa with an increase in the welding energy to 650 J and 800 J. This means that the joint quality improved from 450 J to 650 J and 800 J. In terms of LSS1 and LSS2, it can be confirmed that the efficiency and quality of the joints welded at 650 J and 800 J with FED are almost the same. Furthermore, the effectiveness of FED is confirmed from the viewpoint of the quality of the joints because LSS2 of the joints with FED is higher than that of the joints without it at 650 J and 800 J. Although the actual welded area of the joints without FED appears to be larger than that of the joints with FED, the joint quality seems to be insufficient. The difference in the fracture mechanisms for these joints is investigated in the next subsection. Here, the scatters of LSS2 for the joints with FED are larger than that for the joints without FED, although the scatters of LSS1 are almost equal in all joints. This is because that the scatters of LSS2 include the scatters of the maximum load and the welded area, while those of LSS1 are affected by only the maximum load.

Next, Fig. 22 shows LSS2 of the twill woven laminate joints without and with FED. For both the joints without and with FED, LSS2 mildly increased to around 30.0 MPa as the welding energy increased. However, clear difference of LSS2 between the joints without and with FED cannot be found, in contrast to LSS1. This means that FED works to expand the welded area and improve LSS1, but the actual strength of the joints is not

improved so much by FED. This results in an LSS2 that is similar to that of the joints without FED.

3.1.5. Welding surface observations

Figs. 23 and 24 show the fracture surfaces of the cross-ply laminate joints without and with FED observed by a digital optical microscope. As shown in Figs. 23(a) and 24(a), the exposed fibers were clearly observed at the welding areas. Micrograph images of the fracture surface of the joints without FED are shown in Figs. 23(b)-(d). At the edges of the welding area (points A and C), the fibers were fractured widely, and step-like fracture surfaces were observed. By contrast, fractured fibers were rarely found and the fracture surface was relatively flat at the middle part of the welding area (point B).

On the other hand, the fracture surface of the joints with FED, as shown in Figs. 24(b)-(d), was different from that of the joint without FED. Although the flat fracture surface (point E) and the step-like one (point F) occurred at the middle part and the edges of the grip side of the welding area (as in the case without FED), a sloping fracture surface owing to pullout of the fibers was observed at the edge of the free-edge side of the welding area (point D). This is almost the same fracture aspect as that of a mode-I fracture.

From these micrographs, the fracture mechanisms of LSTs for the cross-ply laminate joints are discussed. The fracture mechanism of the joints without FED is shown in Fig. 25. The peeling stress toward the out-of-plane direction of the adherends occurred around the welding area owing to a concentration of the tensile load. In addition, the in-plane tensile and compressive stresses were distributed around the edges of the welding area near the grip and free-edge sides. The fracture of the joints initiated from

the delamination and local buckling of the fibers owing to the out-of-plane peeling and in-plane compressive stresses for both of the adherends (Fig. 25(a)). Then, the crack developed between the fractured areas at the compressive parts of the adherends. As a result, a slanting fracture surface like that in Fig. 25(b) was generated in the cross-ply laminate joints without FED. The same stress distribution occurred in the joints with FED, as indicated in Fig. 26. However, the fracture of the fibers occurred at only one side of the adherend and extended inside of it because the strength of FED layer and that of the interface between the already molded FED/adherend were sufficiently high, and the stress concentration at the other side of the adherend was weakened by FED. Thus, the crack growth accompanying the pullout of the fibers progressed at one side of the adherend, and the trapezoidal fracture surface occurred as illustrated in Fig. 26(b). To confirm the stress distribution mentioned above, the elastic finite element analyses were performed. The numerical models which had the same dimensions as the LST specimens with and without FED were used. In the numerical models, each layer of the prepregs and FED was modeled by one layer of the elements. The one end was fixed, and the 1.0 mm nodal displacement was applied at the other end of the models. The stress distributions around the welded areas are indicated in Figs. 25(c) and 26(c). The tensile and compressive stress distribution similar to Figs. 25(a) and 26(a) can be confirmed qualitatively. In addition, the stress concentration at the interface beween the already molded FED/adherend is weakened by FED as shown in Fig. 26(c).

For the twill woven laminates, however, the fracture surfaces were almost

the same in the cases with and without FED. A typical fracture surface of the twill woven laminate joints with FED is indicated in Fig. 27. Both the fiber bundles parallel to and perpendicular to the tensile direction were broken at the fracture surface of the joints. The micrograph shown in Fig. 28 indicates the fractured fiber bundles perpendicular to the loading direction. The fracture of the joints was initiated from damage to the fiber bundles perpendicular to the loading direction by the shear stress because the shear strength of the carbon fibers was lower than the tensile strength. Thus, it can be assumed that the nonlinearity of the load-displacement curves shown in Fig. 17 was caused by the shear fracture of the fiber bundles and failure of the surrounding matrix resin. Then, the tensile load decreased drastically owing to the tensile fracture of the fiber bundles parallel to the tensile direction.

3.2. Cross tensile test

3.2.1. Load-displacement curve

The typical load-displacement curves of CTTs for the cross-ply laminate joints with three welding energies are shown in Fig. 29. The load-displacement curves without and with FED are indicated by the dotted and solid lines, respectively. Different from the results of the LSTs, a temporary decrease in the loads can be found in some specimens because the failure gradually progressed from the edges of the joints. As in the case with LSTs, however, the maximum loads became high as the welding energy increased to 800 J for the joints with FED, although those of the joints without FED saturated at more than 650 J.

For the twill woven laminates, the load-displacement curves obtained from CTTs are indicated in Fig. 30. The maximum loads increased with higher

welding energies for the specimens with and without FED. This was similar to the results for the LSTs. Moreover, the maximum loads for the joints with FED were also higher than those for the joints without FED, for example, about 0.8 kN and 1.4 kN for the joints without and with FED welded at 650 J. This is the same mechanism mentioned in the previous subsection, wherein the melting resin from FED can fill out the roughness of the adherend surfaces.

3.2.2. Cross tensile strength 1

From the results of the CTTs, CTS1 was calculated for the cross-ply laminate joints without and with FED. This is shown in Fig. 31. As shown in the figure, CTS1 without FED almost saturated at around 1.2 MPa at 650 J. On the other hand, CTS1 of the cross-ply laminate joints with FED barely increased from 650 J and 800 J. Although the strength of the joints welded at 650 J was twice as high as that at 450 J, an additional welding energy of more than 650 J did not significantly improve the joint strength, but the depth of indentation was increased, for example 1.07 mm (650 J) to 1.22 mm (800 J) in the case of the joints with FED. This is the same tendency as LSS1 of the cross-ply laminate joints. Moreover, FED was not instructive in improving the welding efficiency of the cross-ply laminate joints because the tensile strength of the joints with and without FED was approximately the same, as with LSS1. As a result, it is supposed that 650 J is the efficient welding energy in the cases with and without FED.

Fig. 32 also shows CTS1 for the twill woven laminate joints. From the results of the joints without FED, CTS1 clearly increased with an increase in the welding energy. CTS1 for the joints with FED also increased as the

welding energy increased from 650 J to 800 J, although CTS1 welded at 450 J and 650 J showed similar values. From the results of CTS1 for these two types of joints, the effectiveness of FED can be confirmed for all welding energies, especially for 450 J. The most efficient welding condition for the twill woven laminate joints is thus considered to be 800 J with FED.

3.2.3. Cross tensile strength 2

In the same manner, CTS2 of the cross-ply and twill woven laminate joints was also estimated. CTS2 of the cross-ply laminate joints is shown in Fig. 33. As for the joints without FED, CTS2 was almost equal in all welding energies. This means that an increase in the welding energy only expands the real welded area and improves the welding efficiency. Although LSS2 of the cross-ply laminate joints was improved by FED, CTS2 with FED became high as the welding energy increased but did not improve as much as that without FED. It is assumed that this tendency was caused by the difference in the fracture mechanisms between LSTs and CTTs. For LSTs, the fracture mechanism was changed by FED, and LST2 improved. By contrast, the fracture surfaces for the joints with and without FED on CTTs were almost the same, as mentioned in the following subsection. This resulted in a similar CTS2 in the cases with and without FED. Thus, FED improved the welding quality of the joints only for LSS2. Concerning CTS1, CTS2, and the depths of the indentations at the welding surface, the sufficient welding energy of the cross-ply laminate joints for CTTs is determined as 650J in the cases of with and without FED.

For the twill woven laminate joints, CTS2 without and with FED is indicated in Fig. 34. Similar to the cross-ply laminate joints without FED, the

joints without FED welded at 450 J, 650 J, and 800 J achieved almost the same strength: approximately 5.0 MPa. This implies that a difference in the welding energy is not related to improvements in the joint quality without FED. The strengths with FED welded at 650 J and 800 J are higher than those without FED. It is thus confirmed that the FED improves not only the welding efficiency but also the welding quality of the twill woven laminate joints. Maximum CTS2 was obtained in the welding condition of 650 J with FED. However, from these results, the most suitable welding energy is 800 J in the twill woven laminate joints because the dispersion of CTS2 at 800 J is smaller than that at 650 J, and CTS1 (that is an ultimate load) at 800 J was higher than that at 650 J.

3.2.4. Welding surface observations

As for CTTs of the cross-ply laminate joints, similar fracture surfaces were observed regardless of whether they had FED. It is assumed that the same fracture mechanism resulted in similar tensile strengths of the joints with and without FED. Fig. 35 shows the typical fracture surface of the cross-ply laminate joints with FED. As shown in the figure, a fracture of the thermoplastic resin and interfacial debonding between the fibers and the resin widely occurred, while fractured fibers were rarely found. In particular, a characteristic fracture surface similar to saw blades caused by plastic deformation of the resin can be observed. This result suggests that the mechanical property of the resin has an important role in improving the tensile strength of the cross-ply laminate joints.

Figs. 36 and 37 show the typical fracture surface of twill woven laminate joints with and without FED. Different from the results for the cross-ply

laminate joints, the fractured fibers on the fracture surface of the twill woven laminate joints were clearly observed. Thus, CTS of the twill woven laminate joints had a higher value than that of the cross-ply laminate joints. Moreover, the fracture of the fibers for the joints with FED reached a deeper area of the adherends than the joints without FED. This is the reason that CTS of the twill woven laminate joints increased using FED.

4. Conclusion

This paper investigated the strengths of CFRTP joints by ultrasonic welding in two ways, and revealed the effects of welding energy and FED on the joint strength. The adherends used in this study were cross-ply CFRTP laminates made of unidirectional prepregs and twill woven CFRTP laminates. In the experiments, lap shear tests (LSTs) and cross tensile tests (CTTs) were performed to evaluate the shear and tensile strengths of the joints, respectively. A modified CTT jig and a testing method of CFRTP joints were proposed because CTTs were not standardized for CFRTP laminate joints. In each test, the strengths were calculated using the indicators of "welding efficiency (LSS1 and CTS1)" and "welding quality (LSS2 and CTS2)." Additionally, the fracture surfaces were observed in order to evaluate the fracture mechanisms of the joints. The main conclusions of this paper are summarized as follows:

1. Lap shear tests
    - The welded area and the indentation of the sonotrode were investigated for each welding energy. For the cross-ply laminate joints,

the welded area of the joints with FED was smaller than that of the joints without FED, but the indentation for the joints without FED became deep as the welding energy increased compared with that for the joints with FED, especially at 800 J. By contrast, the welded area of the twill woven laminate joints increased owing to FED, and the indentation was almost equal for all welding conditions.

- The load-displacement curves of the cross-ply laminate joints showed linear behavior, and the maximum load was the same (about 4.0 kN at 650 J and 800 J) for the cases with and without FED. For the twill woven laminates, however, the maximum load increased at higher welding energies and in the case with FED.
- For the cross-ply laminate joints, LSS1 increased to 650 J and almost saturated at higher than 650 J, around 7.0 MPa for the joints with and without FED. By contrast, a maximum LSS1 was obtained at 800 J for the twill woven laminate joints. Moreover, LSS1 of the twill woven laminate joints with FED was extremely high compared with that of the joints without FED, 11.5 MPa and 6.5 MPa, respectively.
- As for LSS2, the shear strength of the cross-ply laminate joints was improved by FED. LSS2 of the cross-ply laminate joints without FED saturated at 25.0 MPa at higher than 450 J, but that of the joints with FED increased to about 40.0 MPa when welded at 650 J and 800 J. LSS2 of the twill woven laminate joints was almost the same around 30.0 MPa for both the joints with and without

FED. This means that FED affects the "welding quality" of the cross-ply laminate joints and the "welding efficiency" of the twill woven ones.

- From the results of fracture surface observations, different fracture modes were found for the cross-ply laminate joints with and without FED. It can be considered that the fracture mode changed and the "welding quality" was improved by FED. In addition, melted resin from FED helped to fill in the surface roughness of the twill woven laminate joints, and this resulted in an advance in the "welding efficiency."

2. Cross tensile tests

- The load-displacement curves for the cross-ply and twill woven laminate joints showed remarkable nonlinear behavior owing to gradual failure progression. The maximum load saturated at higher than 650 J for the cross-ply laminate joints without FED, but increased to 800 J for the joints with an FED (about 0.75 kN). By contrast, the maximum load increased to 1.4 kN for the twill woven laminate joints with FED compared with the joints without FED.

- CTS1 showed a similar tendency as LSS1. CTS1 of the cross-ply laminate joints welded at 650 J and 800 J was approximately equal and was around 1.2 MPa for the cases with and without FED. In the case of the twill woven laminate joints, CTS1 increased gradually as the welding energy increased, and a higher CTS1

was obtained using FED. The maximum CTS1 of the twill woven laminate joints was 2.7 MPa for the cases with FED welded at 800 J.

- The effectiveness of FED on CTS2 was also observed for both the cross-ply and twill woven laminate joints. CTS2 of the cross-ply and twill woven laminate joints with FED increased compared with the joints without FED, but its degree of influence was not as significant as with LSS2.
- Similar fracture surfaces consisting of fractures of the matrix resin and interfacial debonding were observed for the cross-ply laminate joints with and without FED. Therefore, CTS2 for the cross-ply laminate joints with FED did not improve significantly. The fractured area of the twill woven laminate joints, however, was enlarged by using FED, and thus CTS2 with FED increased.

From the experimental results, FED mainly worked to improve LSS2 and CTS2 of the "welding quality." This indicates that the joint strength per unit area is improved by FED for the cross-ply laminate joints. By contrast, for the twill woven laminate joints, FED increased LSS1 and CTS1 of the "welding efficiency," i.e., it enlarged the welded area. It is important to investigate suitable welding conditions which can improve the both "welding efficiency" and "welding quality" in the viewpoint of practical engineering application.

References

[1] Duflou JR, De Moor J, Verpoest I, Dewulf W. Environmental impact analysis of composite use in car manufacturing. CIRP Ann-Manuf Techn 2009;58(1):9-12.

[2] Takahashi J, Ishikawa T. Current Japanese activity in CFRTP for industrial application. In: Proceedings of TexComp-11 Conference. Leuven, September, 2013. p.16-20.

[3] Ishikawa T, Amaoka K, Masubuchi Y, Yamamoto T, Yamanaka A, Arai M, Takahashi J. Overview of automotive structural composites technology developments in Japan. Compos Sci Technol 2018;155:221-246.

[4] Jaeschke P, Herzog D, Haferkamp H, Peters C, Herrmann AS. Laser transmission welding of high-performance polymers and reinforced composites - A fundamental study. J Reinf Plast Compos 2010;29(20):3083-3094.

[5] Bayerl T, Duhovic M, Mitschang P, Bhattacharyya D. The heating of polymer composites by electromagnetic induction - A review. Compos Part A-Appl S 2014;57:27-40.

[6] Shi H, Villegas IF, Bersee HEN. Strength and failure modes in resistance welded thermoplastic composite joints: Effect of fibre-matrix adhesion and fibre orientation. Compos Part A-Appl S 2013;55:1-10.

[7] Koutras N, Villegas IF, Benedictus R. Influence of temperature on the strength of resistance welded glass fibre reinforced PPS joints. Compos Part A-Appl S 2018;105:57-67.

[8] Villegas IF, van Moorleghem R. Ultrasonic welding of carbon/epoxy and carbon/PEEK composites through a PEI thermoplastic coupling layer. Compos Part A-Appl S 2018;109:75-83.

[9] Lionetto F, Morillas MN, Pappadà S, Buccoliero G, Villegas IF, Maffezzoli A. Hybrid welding of carbon-fiber reinforced epoxy based composites. Compos Part A-Appl S 2018;104:32-40.

[10] Krüger S, Wagner G, Eifler D. Ultrasonic welding of material/composite joints. Adv Eng Mater 2004;6(3):157-159.

[11] Lionetto F, Balle F, Maffezzoli A. Hybrid ultrasonic spot welding of aluminum to carbon fiber reinforced epoxy composites. J Mater Process Technol 2017;247:289-295.

[12] Van Wijk H, Luiten GA, Van Engen PG, Nonhof CJ. Process optimization of ultrasonic welding. Polym Eng Sci 1996;36(9):1165-1176.

[13] Zhao T, Broek C, Palardy G, Villegas IF, Benedictus R. Towards robust sequential ultrasonic spot welding of thermoplastic composites: Welding process control strategy for consistent weld quality. Compos Part A-Appl S 2018;109:355-367.

[14] Villegas IF. In situ monitoring of ultrasonic welding of thermoplastic composites through power and displacement data. J Thermoplast Compos Mater 2015;28(1):66-85.

[15] Villegas IF. Strength development versus process data in ultrasonic welding of thermoplastic composites with flat energy directors and its

application to the definition of optimum processing parameters. Compos Part A-Appl S 2014;65:27-37.

[16] Potente H. Ultrasonic welding – Principles and theory. Mater Design, 1988;5(5):62-72.

[17] Chuah YK, Chien LH, Chang BC, Liu SJ. Effects of the shape of the energy director on far-field ultrasonic welding of thermoplastics. Polym Eng Sci 2000;40(1):157-167.

[18] Chan WX, Ng SH, Li KHH, Park WT, Yoon YJ. Micro-ultrasonic welding using thermoplastic-elastomeric composite film. J Mater Process Technol 2016;236:183-188.

[19] Villegas IF, Bersee HEN. Ultrasonic welding of advanced thermoplastic composites: An investigation on energy-directing surfaces. Adv Polym Technol 2010;29(2):112-121.

[20] Villegas IF, Grande BV, Bersee HEN, Benedictus R. A comparative evaluation between flat and traditional energy directors for ultrasonic welding of CF/PPS thermoplastic composites. Compos Interfaces 2015;22(8):717-729.

[21] Levy A, Le Corre S, Chevaugeon N, Poitou A. A level set based approach for the finite element simulation of a forming process involving multiphysics coupling: Ultrasonic welding of thermoplastic composites. Eur J Mech A-Solids 2011;30(4):501-509.

[22] Levy A, Le Corre S, Villegas IF. Modeling of the heating phenomena in

ultrasonic welding of thermoplastic composites with flat energy directors. J Mater Process Technol 2014;214(7):1361-1371.

[23] Zhao T, Palardy G, Villegas IF, Rans C, Martinez M, Benedictus R. Mechanical behaviour of thermoplastic composites spot-welded and mechanically fastened joints: A preliminary comparison. Compos Part B-Eng 2017;112:224-234.

[24] Radakovic DJ, Tumuluru M. An evaluation of the cross-tension test of resistance spot welds in high-strength dual-phase steels. Weld J 2012;91(1):8s-15s.

[25] Haque R, Durandet Y. Strength prediction of self-pierce riveted joint in cross-tension and lap-shear. Mater Design 2016;108:666-678.

[26] Szlosarek R, Karall T, Enzinger N, Hahne C, Meyer N. Mechanical testing of flow drill screw joints between fibre-reinforced plastics and metals. Mater Test 2013;55(10):737-742.

[27] Kairouz KC, Matthews FL. Strength and failure modes of bonded single lap joints between cross-ply adherends. Composites 1993;24(6):475-484.

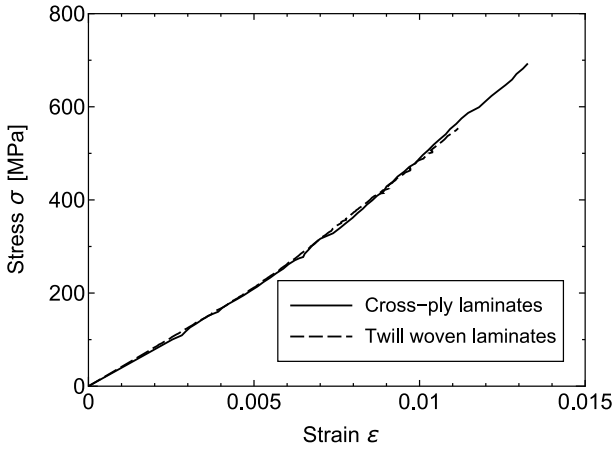

Figure 1: Relation between stress and strain of cross-ply and twill woven laminates.

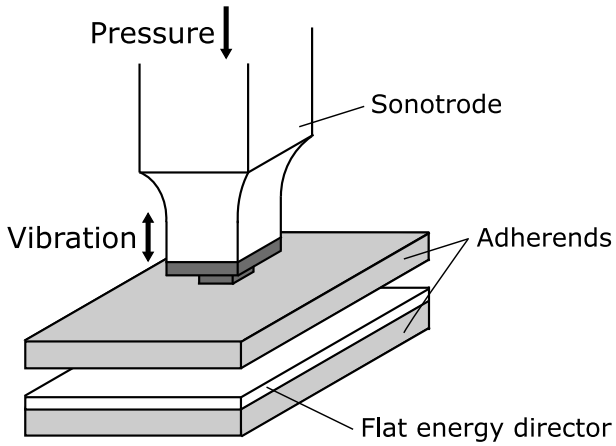

Figure 2: Image of ultrasonic welding with flat energy director.

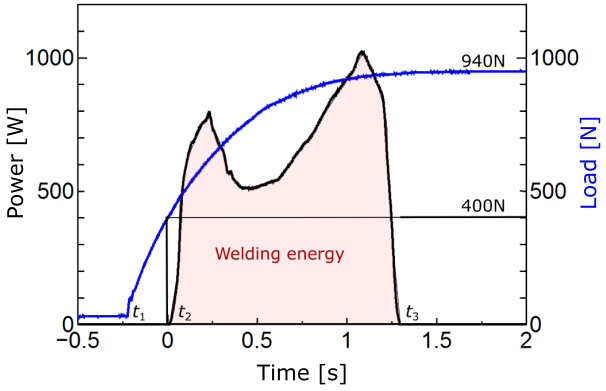

Figure 3: Welding sequence.

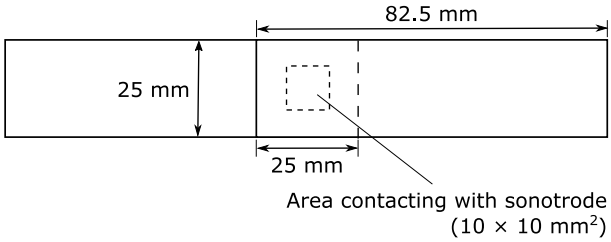

Figure 4: Specimen diagram of lap shear test.

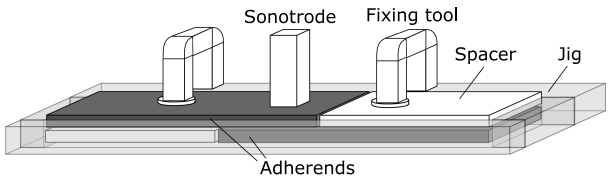

Figure 5: Jig image for manufacturing specimens for lap shear test.

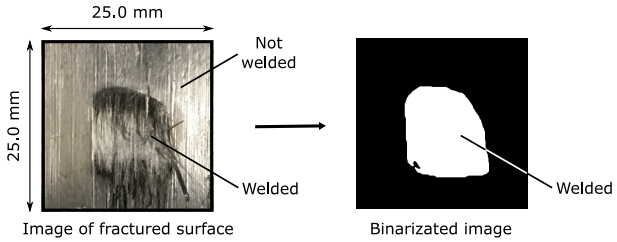

Figure 6: Calculation method for actual welded area.

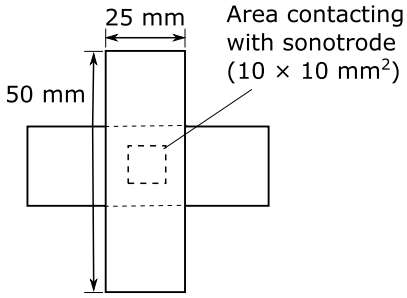

Figure 7: Specimen diagram of cross tensile test.

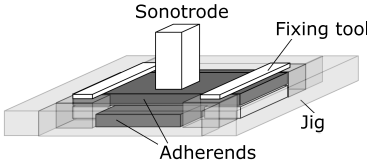

Figure 8: Jig image for manufacturing specimens for cross tensile test.

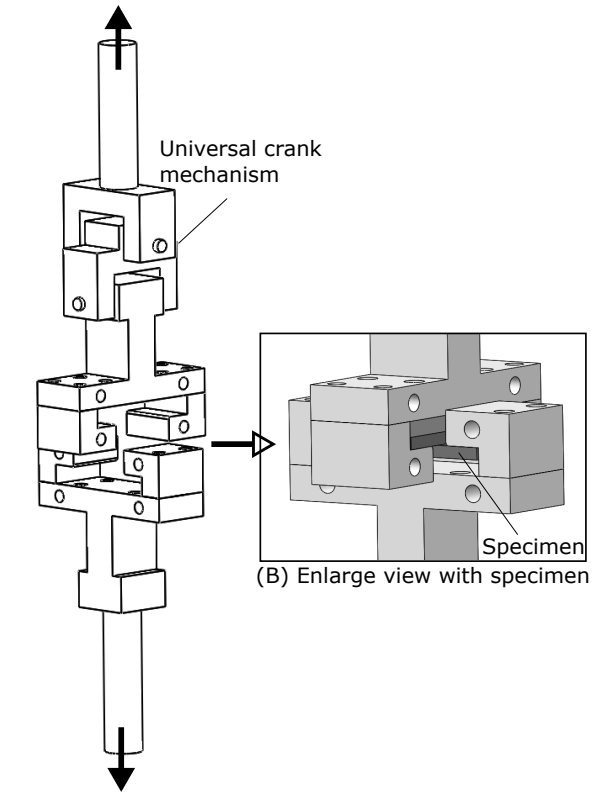

Figure 9: Tensile jig for cross tensile test.

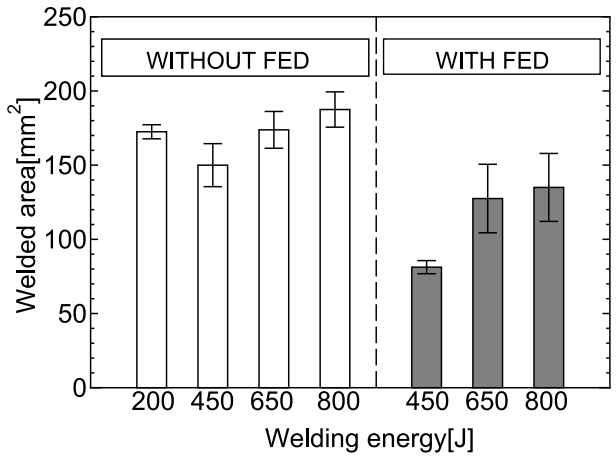

Figure 10: Welded area of cross-ply laminate joints for lap shear tests.

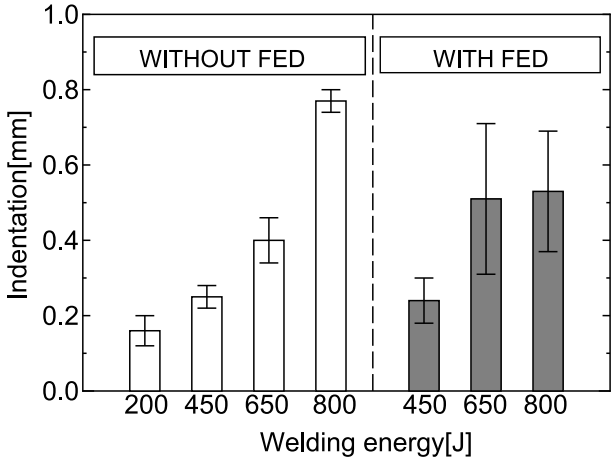

Figure 11: Indentation of cross-ply laminate joints for lap shear tests.

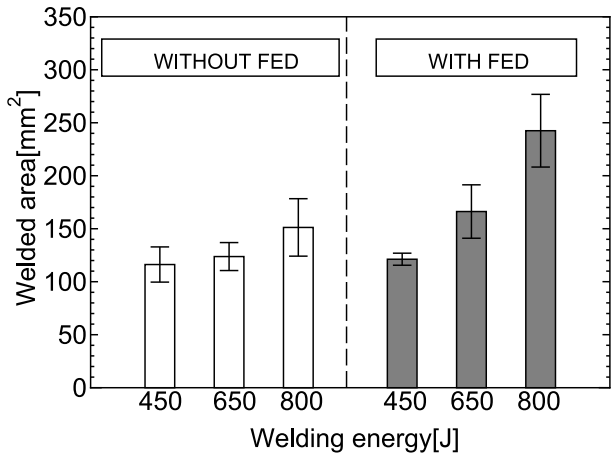

Figure 12: Welded area of twill woven laminate joints for lap shear tests.

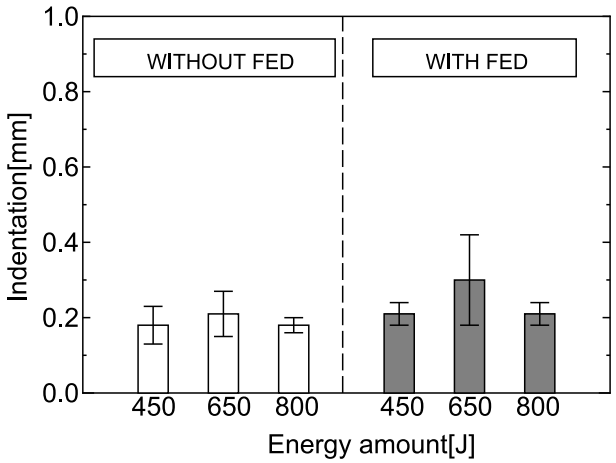

Figure 13: Indentation of twill woven laminate joints for lap shear tests.

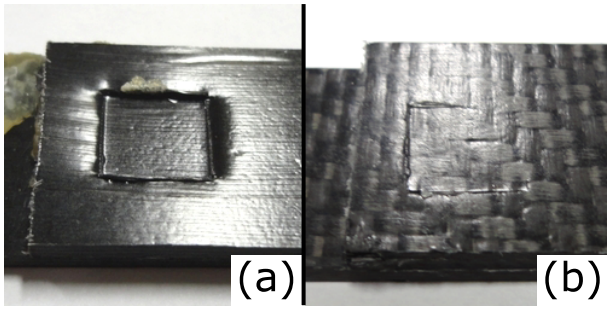

Figure 14: Indentation by sonotrode tip; (a) cross-ply and (b) twill-woven laminate joints without flat energy director welded by 800 J.

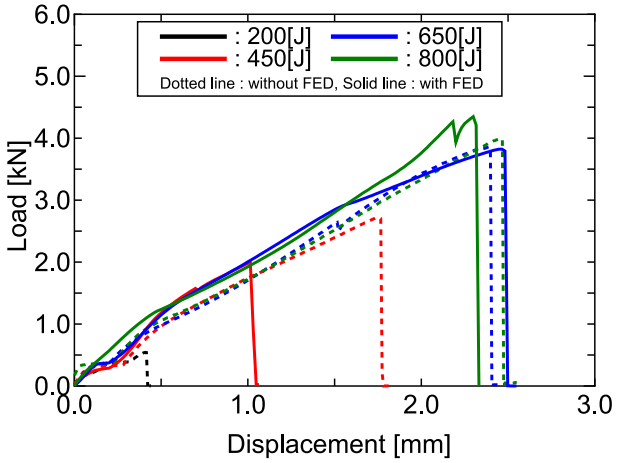

Figure 15: Representative load-displacement curves of lap shear tests for cross-ply laminate joints.

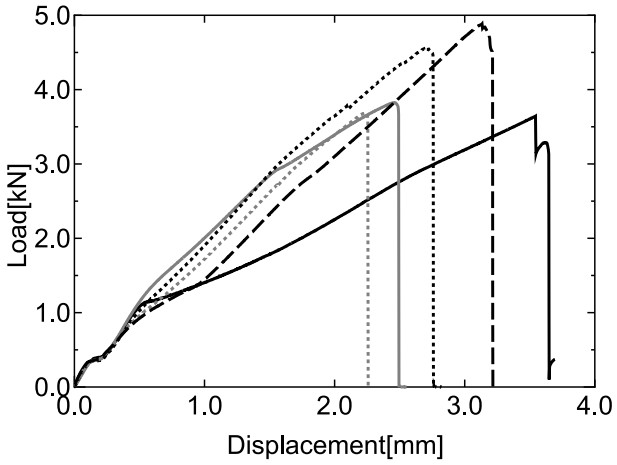

Figure 16: Individual load-displacement curves of lap shear tests for cross-ply laminate joints with flat energy director welded by 650 J.

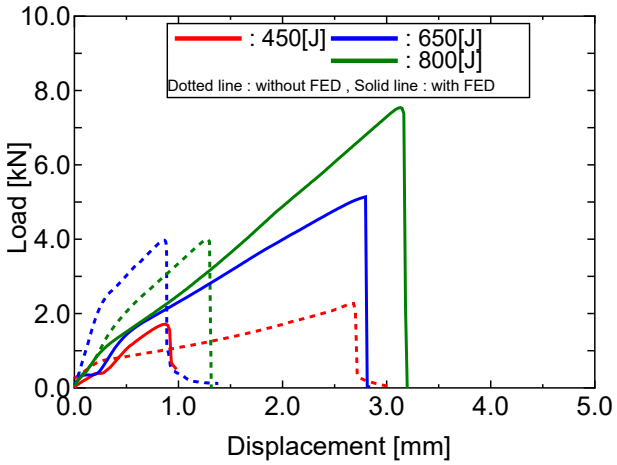

Figure 17: Representative load-displacement curves of lap shear tests for twill woven laminate joints.

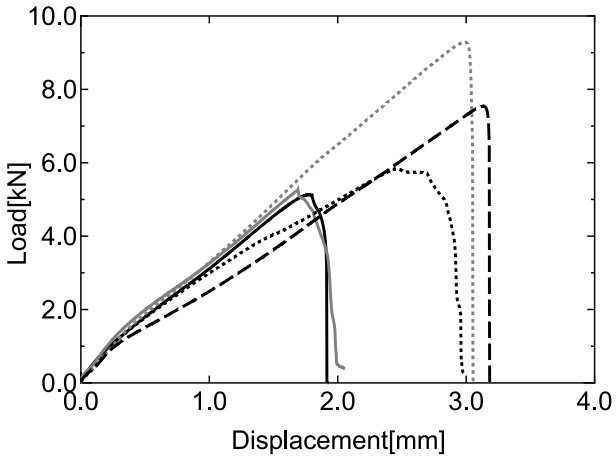

Figure 18: Individual load-displacement curves of lap shear tests for twill woven laminate joints with flat energy director welded by 800 J.

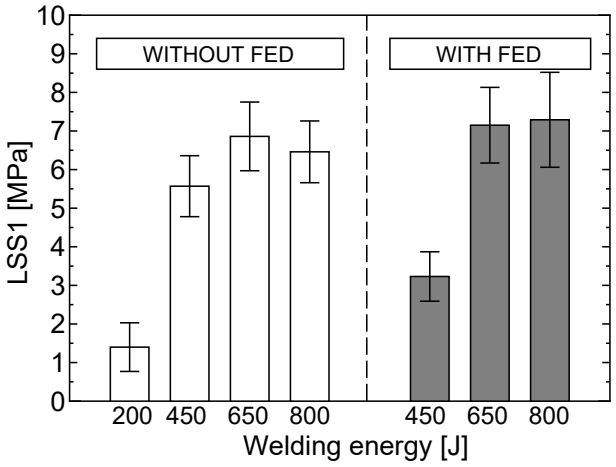

Figure 19: Lap shear strength 1 for cross-ply laminate joints.

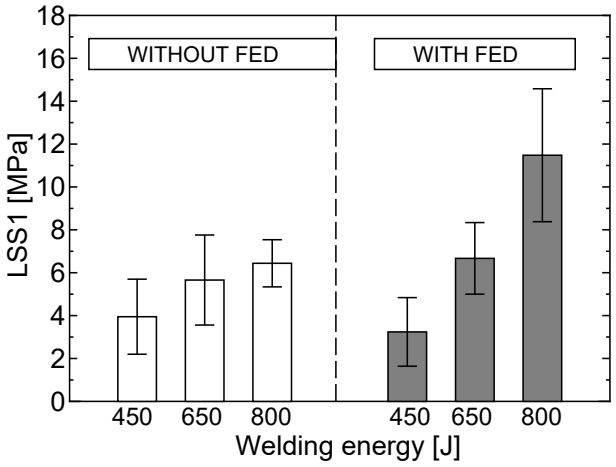

Figure 20: Lap shear strength 1 for twill woven laminate joints.

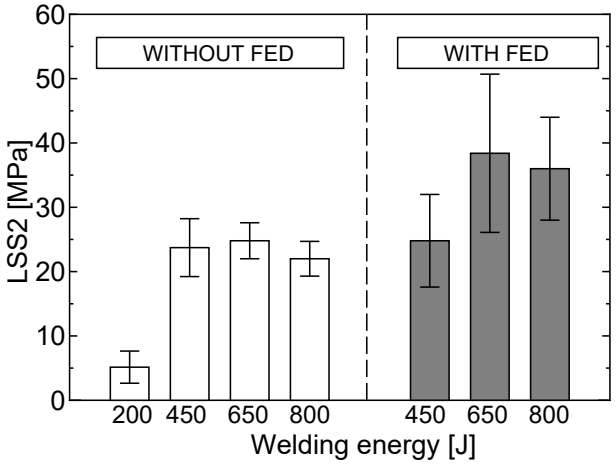

Figure 21: Lap shear strength 2 for cross-ply laminate joints.

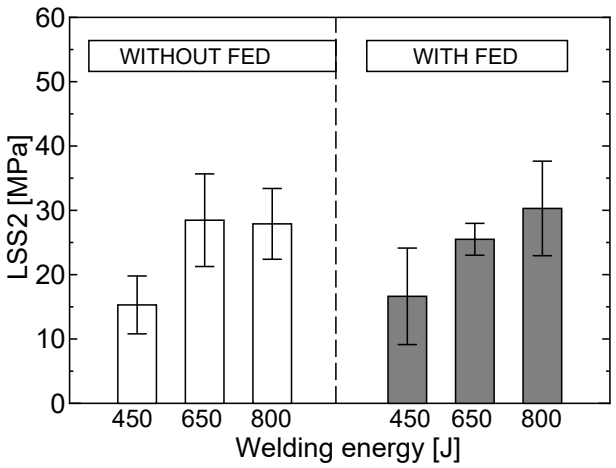

Figure 22: Lap shear strength 2 for twill woven laminate joints.

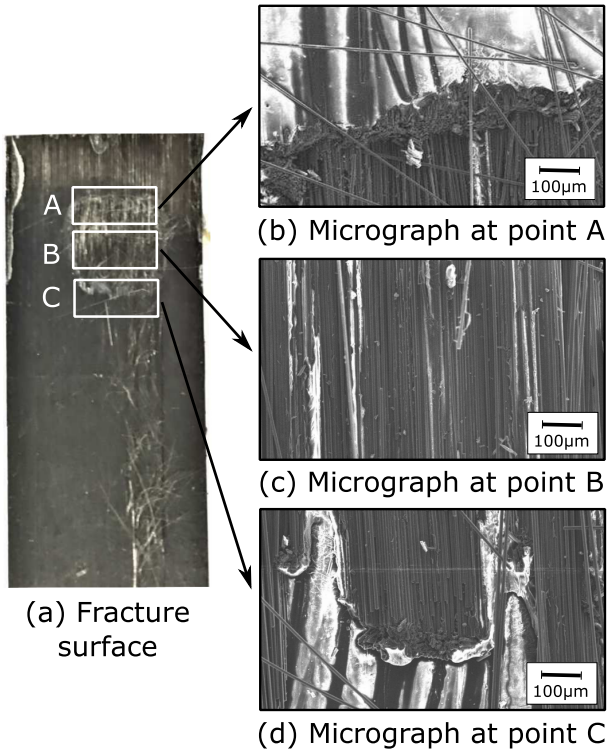

Figure 23: Fracture surfaces of cross-ply laminate joint without flat energy director of lap shear test.

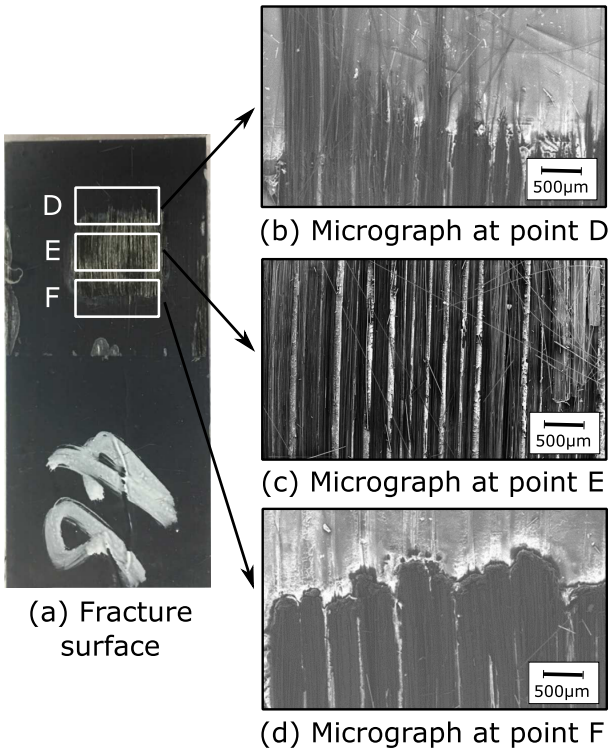

Figure 24: Fracture surfaces of cross-ply laminate joint with flat energy director of lap shear test.

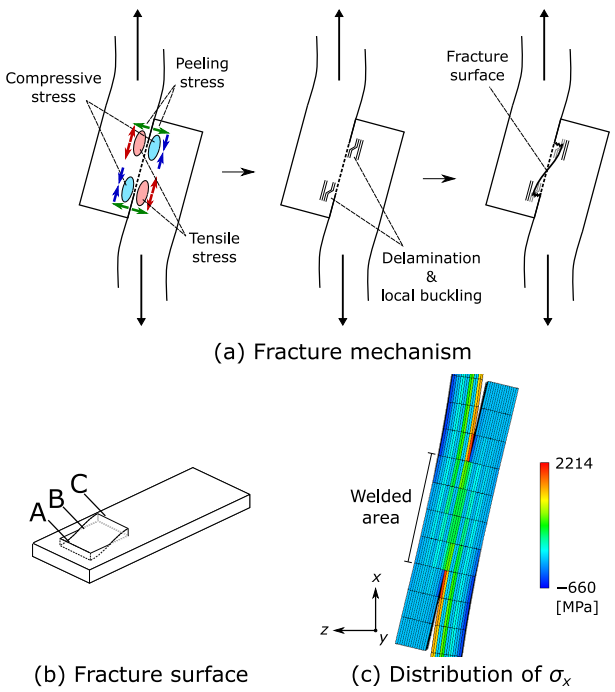

Figure 25: Fracture mechanism of cross-ply laminate joint without flat energy director.

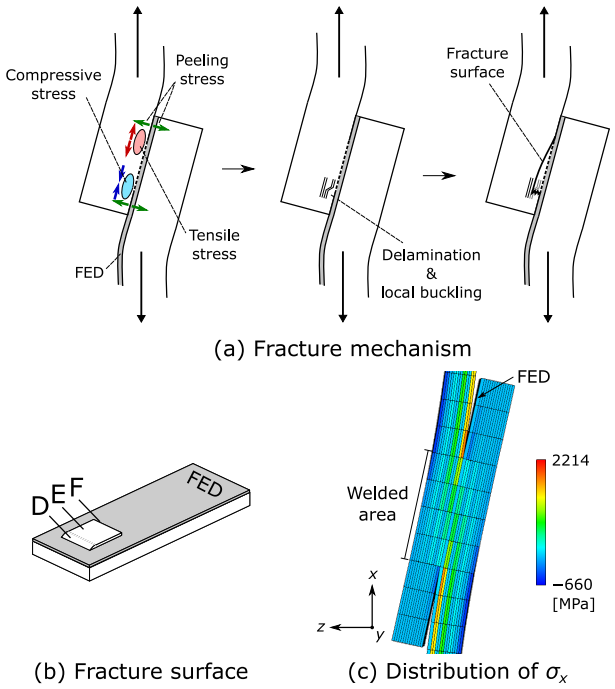

Figure 26: Fracture mechanism of cross-ply laminate joint with flat energy director.

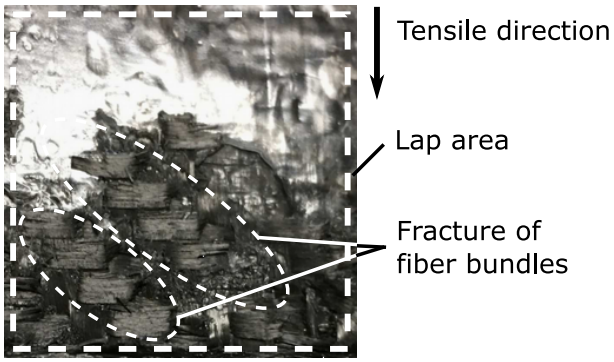

Figure 27: Fracture surface of twill woven laminate joint with flat energy director of lap shear test.

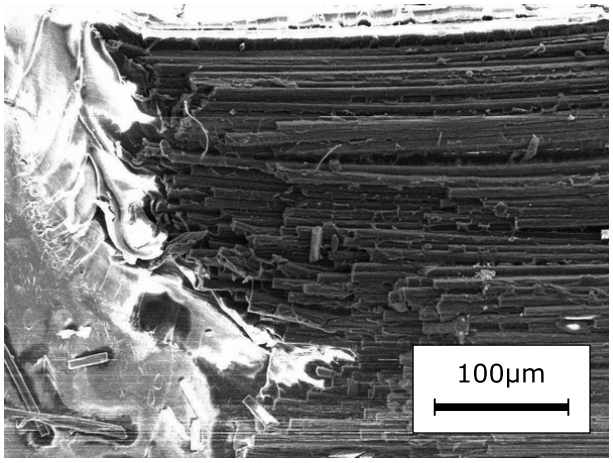

Figure 28: Micrograph of fractured fiber bundle perpendicular to tensile direction.

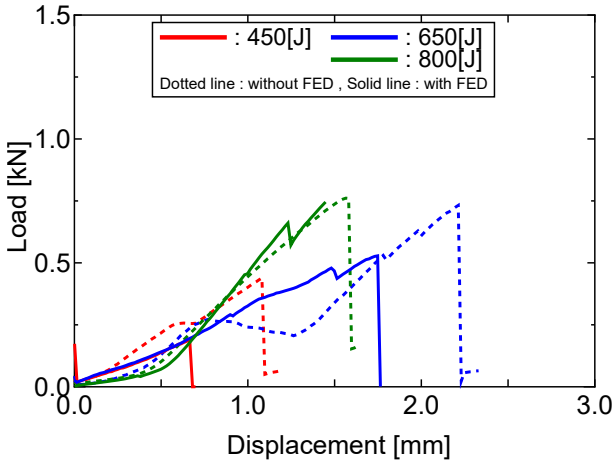

Figure 29: Load-displacement curves of cross tensile tests for cross-ply laminate joints.

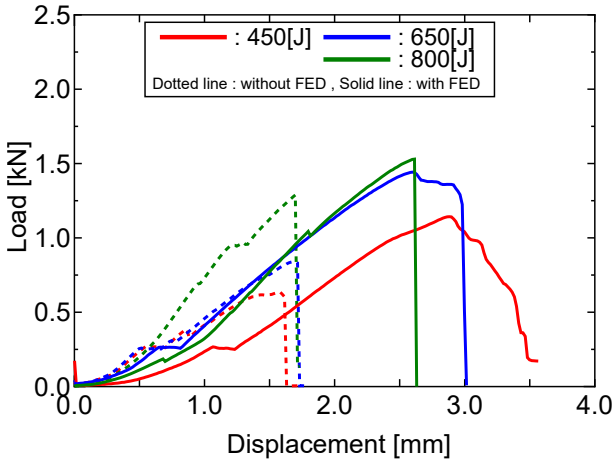

Figure 30: Load-displacement curves of cross tensile tests for twill woven laminate joints.

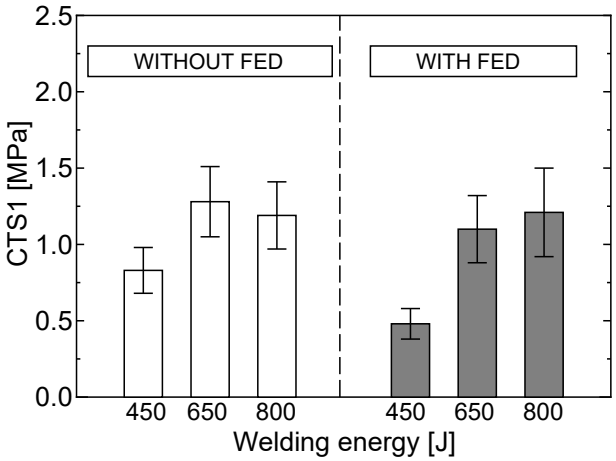

Figure 31: Cross tensile strength 1 for cross-ply laminate joints.

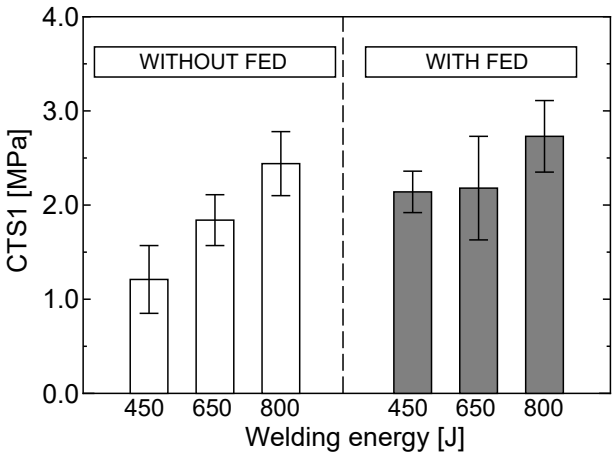

Figure 32: Cross tensile strength 1 for twill woven laminate joints.

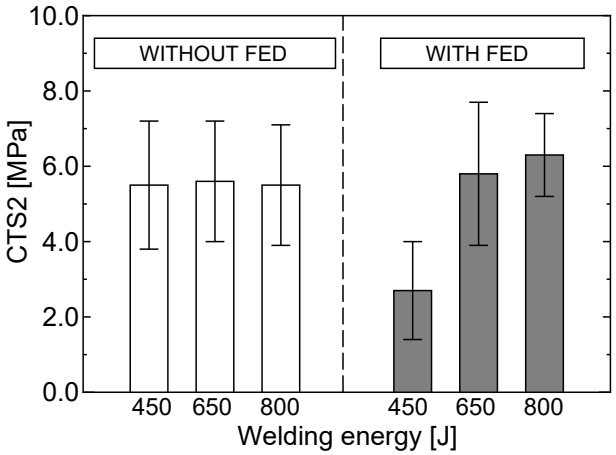

Figure 33: Cross tensile strength 2 for cross-ply laminate joints.

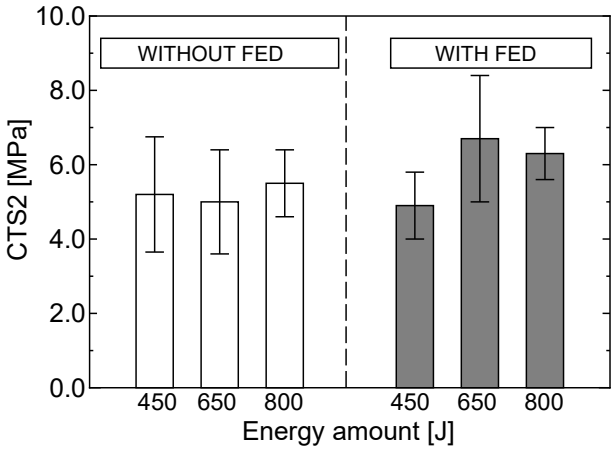

Figure 34: Cross tensile strength 2 for twill woven laminate joints.

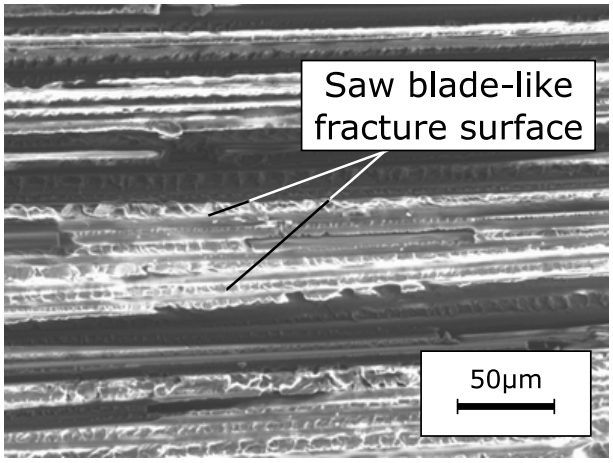

Figure 35: Fracture surface of cross-ply laminate joint with flat energy director of cross tensile test.

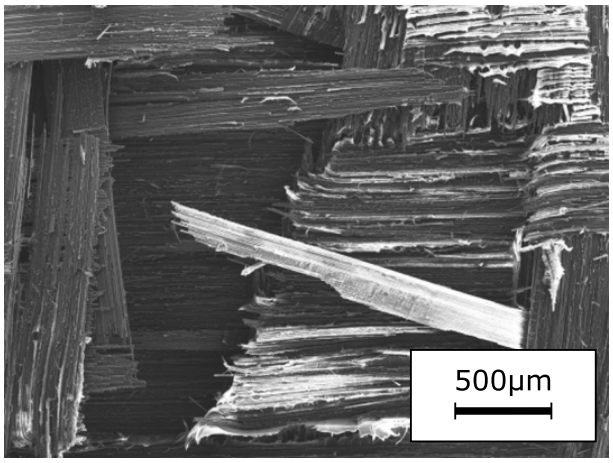

Figure 36: Fracture surface of twill woven laminate joint with flat energy director of cross tensile test.

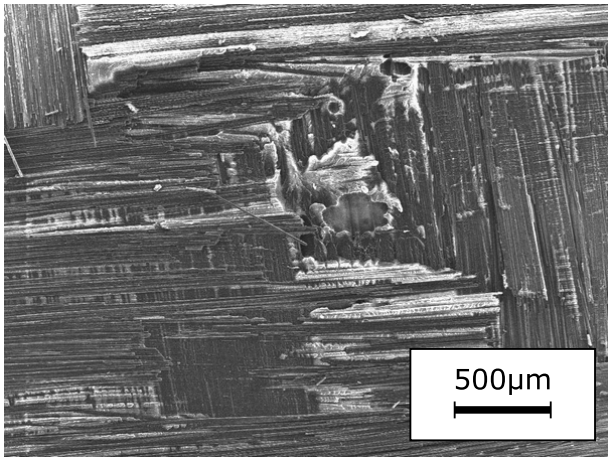

Figure 37: Fracture surface of twill woven laminate joint without flat energy director of cross tensile test.